https://doi.org/10.5194/egusphere-2024-2625
Preprint. Discussion started: 18 September 2024

Combining commercial microwave links and weather radar for classification of dry snow and rainfall

Erlend Øydvin[1], Renaud Gaban[1, 5], Jafet Andersson[2], Remco van de Beek[2], Mareile Astrid Wolff[1, 5], Nils-Otto Kitterød[4], Christian Chwala[3], and Vegard Nilsen[1]

[1]Faculty of Science and Technology, Norwegian University of Life Sciences, Ås, Norway
[2]Swedish Meteorological and Hydrological Institute (SMHI), 601 76 Norrköping, Sweden
[3]Institute of Meteorology and Climate Research, Karlsruhe Institute of Technology, Campus Alpin, Garmisch-Partenkirchen, Germany
[4]Faculty of Environmental Sciences and Natural Resource Management, Norwegian University of Life Sciences, Ås, Norway
[5]Norwegian Meteorological Institute, Oslo, Norway

Correspondence: Erlend Øydvin (erlend.oydvin@nmbu.no)

Abstract. Differentiating between snow and rainfall is crucial for hydrological modeling and understanding. Commercial Microwave Links (CMLs) can provide accurate rainfall estimates for liquid precipitation, but show minimal signal attenuation during dry snow events, causing the CML time series during these periods to resemble non-precipitation periods. Weather radars can detect precipitation also for dry snow, yet, they struggle to accurately differentiate between precipitation types. This study introduces a new approach to improve rainfall and dry snow classification by combining weather radar precipitation detection with CML signal attenuation. Specifically, events where the radar detects precipitation, but the CML does not, are classified as dry snow. As a reference method we use weather radar, with the precipitation type identified by the dew point temperature at the CML location. Both methods were evaluated using ground measurements from disdrometers within 8 km of a CML, analysing data from 550 CMLs in December 2021 and 435 CMLs in June 2022. Our results show that using CMLs can enhance the classification of dry snow and rainfall, presenting an advantage over the reference method. Further, our research provides valuable insights into how precipitation at temperatures around zero degrees, such as sleet or wet snow, can affect CMLs, contributing to a better understanding of CML applications in colder climates.

1 Introduction

The precipitation phase is crucial for hydrological processes in cold regions (Loth et al., 1993). Understanding the type of precipitation aids in applications such as adjusting rain gauges for wind undercatch (Kochendorfer et al., 2022) and modeling hydrological responses like flooding. Moreover, specific precipitation conditions, like freezing rain, can disrupt power lines and impede traffic, while snow can cause transportation blockages. It's also noteworthy that rain-on-snow events have been associated with significant flooding (McCabe et al., 2007).

The formation of precipitation is a complex process. In the high and mid-latitudes, most precipitation originates from mixed-phase or cold clouds, i.e. clouds containing ice (Stewart et al., 2015). The ice crystals grow in size and mass through different micro-physical mechanisms such as vapor deposition and riming, until they reach a sufficient mass to sediment out of the cloud

https://doi.org/10.5194/egusphere-2024-2625
Preprint. Discussion started: 18 September 2024

base (Stewart, 1992). A necessary condition for a cloud to generate solid phase-precipitation is that its temperature is negative. Unless the temperature of the layer of atmosphere underneath the cloud remains below zero degrees, the precipitating ice will start melting before reaching the ground (Lamb and Verlinde, 2011). The melting process is not instantaneous and an ice particle can fall hundreds of meters before melting completely. Therefore, originally solid precipitation can reach the ground in any intermediate state between solid and liquid, depending on the height of the zero-degree isotherm (Paulson and Al-Mreri, 2011; Harpold et al., 2017). The melting process is also influenced by other elements of the atmospheric conditions. Specifically, the stability of the atmosphere and the atmospheric humidity profile have a significant influence because the liquid water formed from melting of ice will tend to evaporate in dry conditions, cooling the atmosphere in turn and hampering further melting (Harder and Pomeroy, 2013). Atmospheric conditions that determine the precipitation phase can change relatively quickly. For instance, a study by Marks et al. (2013) observed a significant increase of the height of the melting layer within the same precipitation event. Determining the precipitation phase at the ground level is therefore difficult and models predicting the precipitation phase typically need to be calibrated and validated against measurements (Harpold et al., 2017).

There are several ways of determining the precipitation phase using ground based observations. For example, Marks et al. (2013) used a combination of a tipping bucket rain gauge and a heated weighing gauge. During rain, the devices record similar amounts, but when it snows, the snow clogs the funnel of the tipping bucket, leaving only the weighing gauge to record precipitation. Other studies, such as Matsuo et al. (1981), used human observers to directly observe precipitation phase. More advanced methods include using weather radars, especially with dual polarization, to estimate and classify precipitation phase (Grazioli et al., 2015; Chandrasekar et al., 2013). Disdrometers also estimate precipitation phase based on the physical properties of hydrometeors (size and fall velocity), with semi-empirical knowledge of how these properties vary with type (Löffler-Mang and Joss, 2000; Yuter et al., 2006). However, each method has its own limitations. Rain gauges, providing point measurements, have limited spatial representation and can be affected by wind induced errors (Førland et al., 1996; Nešpor and Sevruk, 1999; Kochendorfer et al., 2022; Wolff et al., 2015). Human observations can be subjective and aren't suitable for continuous high frequency monitoring. Dual polarized weather radar can suffer from beam blockage and has difficulty linking the estimated precipitation type to ground measurements (Harpold et al., 2017; Elmore, 2011). Like rain gauges, disdrometers are limited in spatial representation and can experience errors such as splashing of drops against nearby structures, drops falling on the edge of the measuring area, and wind altering drop trajectories (Friedrich et al., 2013).

Precipitation phase estimation often employs a temperature model. This involves modeling the rain-snow transition based on temperature using for instance a single temperature threshold to separate rain and snow, or two thresholds that define mixed precipitation in between the two thresholds (Kienzle, 2008). Jennings et al. (2018) found that, when using a single temperature threshold, the threshold separating rain from snow varies geographically, ranging from -0.4 to 2.4 for most stations and with colder thresholds near the coast and warmer thresholds in mountains. They also found that models incorporating humidity performed better than models considering air temperature alone, which is also confirmed by other studies (Matsuo et al., 1981). Other studies again have not observed any benefit of including humidity (Leroux et al., 2023). One common measure combining humidity and temperature is the dew point temperature, which is the temperature at which air becomes saturated with water vapor at the current water content (Lawrence, 2005). This measure can provide important insights into the atmospheric

https://doi.org/10.5194/egusphere-2024-2625
Preprint. Discussion started: 18 September 2024

conditions and aids in classifying precipitation types (Feiccabrino, 2020; Harder and Pomeroy, 2013, 2014). However, even if temperature and humidity are combined to classify precipitation types, there is still a large degree of uncertainty. Harpold et al. (2017) suggest that current phase transition models are too simple to capture the process, especially in complex terrain. They suggest, for instance, to improve this by better use of other atmospheric information and enhancing the validation network with ground measurements such as disdrometers.

CMLs are radio links between radio communication towers. In the mid-2000s, it was demonstrated by Messer et al. (2006) and Leijnse et al. (2007) that CMLs can be used to estimate rainfall. This is due to the relationship between signal attenuation and rainfall intensity. At around 30 GHz, the relation is close to linear, making it easier to estimate the average rainfall intensity along the CML path. Among other applications, CMLs have been used to estimate countrywide rainfall (Graf et al., 2020; Overeem et al., 2016), transboundary rainfall fields (Blettner et al., 2023) and CMLs have proven useful for estimating runoff in urban hydrology (Pastorek et al., 2023). A crucial step in CML rainfall estimation is the detection of rainfall, often called wet periods, in the CML time series. There are several ways of doing this, for instance by classifying a period as wet when the standard deviation of a moving window is larger than a predefined threshold (Schleiss et al., 2013; Graf et al., 2020), by using pre-trained classification methods (Polz et al., 2020; Øydvin et al., 2024) or by including information from nearby CMLs (Overeem et al., 2013). It is also possible to use weather radar to estimate the CML wet period as done in Overeem et al. (2016).

Classification of precipitation types other than rain using CMLs has previously been investigated by Cherkassky et al. (2014). The authors used the fact that snow, sleet, and rainfall are affected differently by different CML frequencies. Thus, by using three CMLs operating at different frequencies in the same area, they were able to distinguish periods of wet snow and rainfall, albeit only for two precipitation events where each lasted for three days. Ostrometzky et al. (2015) expanded on this study by using four CMLs operating at different frequencies and clustered at a single path to estimate the precipitation amounts generated by rainfall and wet snow. The study investigated four precipitation events lasting a total of 16 days. A limitation of both of these studies is that they focus on a low number of CMLs over a few days. It is not known how well these methods generalize to longer time series and larger CML networks.

Not many studies have focused on how CMLs are affected by colder climates. Graf et al. (2020) and Overeem et al. (2016) reported that CMLs tend to overestimate the precipitation amount during winter months. Both attributed this overestimation to wet snow. Paulson and Al-Mreri (2011) reports that wet snow can induce up to four times the attenuation compared to rainfall, leading to potential overestimation of CML rainfall due to the larger size of the wet snow particles. Dry snow, on the other hand, is known to cause signal attenuation so low that it cannot be detected by CMLs (Pu et al., 2020).

In this study, we explore the viability of classifying dry snow by exploiting the fact that dry snow causes unnoticeable attenuation in the CML data. This is done by first using weather radar to detect precipitation and then the precipitation type is classified based on whether the CML detects rainfall or not.

https://doi.org/10.5194/egusphere-2024-2625
Preprint. Discussion started: 18 September 2024

2 Methods

2.1 CML data

The CML dataset was provided by Ericsson and consists of 2777 CMLs spread out across Norway. Each CML records the transmitted and received signal strength every minute for data from two months: December 2021 and June 2022. The total loss (TL) was computed by subtracting the received signal strength from the transmitted signal strength. In our dataset, there were some outliers where the transmitted signal strength was less than -50 dBm. These signals produced negative TL values, which is probably due to recording errors. We opted to completely remove CMLs with transmitted signal strength less than -50 dBm such that the remaining CMLs did not have any negative TL values. We also removed CMLs with more than 15% missing values. This resulted in 2179 CMLs for the summer dataset and 2345 CMLs from the winter dataset. Next, as suggested by Graf et al. (2020), we removed erratic CMLs where the 5 hours moving window standard deviation exceeded the threshold of 2 dBm more than 10 % of the month and noisy CMLs where the 1-hour moving window standard deviation exceeded the threshold of 0.8 dBm more than 33 % of the month. Then CML derived rain rates were estimated using the *pycomlink* software (Chwala et al., 2023) and a similar workflow as described in Graf et al. (2020), Blettner et al. (2023) and Polz et al. (2020). For the classification of wet periods, we used a simple feed-forward neural network (MLP) available from *pycomlink* and described in Øydvin et al. (2024). To account for spatial and temporal differences between the CML and disdrometers, wet periods were extended by 5 minutes forward and 5 minutes backwards in time. Then, a constant baseline for each wet period was estimated by using the average value of the 5 dry time steps before the wet periods and the attenuation due to rain and wet antenna was estimated by subtracting the baseline attenuation from the TL. The attenuation caused by wet antennas was estimated using the method proposed by Leijnse et al. (2008) using the parameters obtained by Graf et al. (2020). Finally, the rainfall rate was computed using the k-R relation, with parameters defined by ITU (2005).

2.2 Radar data

Weather radar data for Norway was downloaded from THREDDS (2024), a data hosting platform for gridded meteorological data run by the Norwegian Meteorological Institute. The radar product is developed from 12 weather radars in Norway. These radars are combined using a Constant Altitude Plan Position Indicator (CAPPI). The final result is a grid with a spatial resolution of 1 km by 1 km and a temporal resolution of 5 minutes. Seaclutter and other large peaks in the data are removed, and groundclutter is identified and corrected using surrounding data. The radar reflectivity (Z [dBz]) is converted to rainfall rates (R [mm/h]) using the Marshall-Palmer relation (Marshall and Palmer, 1948). To make the comparison of the CML-and weather radar data consistent, we used the CML geometry to extract the average radar rainfall rate along the CML using a weighted grid approach provided by *pycomlink*. Then, in line with Polz et al. (2020), time steps with weather radar rainfall rates above 0.1 mm/h were considered wet. To account for spatial and temporal differences between the radar beam and the disdrometer, periods with precipitation as detected by the weather radar were extended by 5 minutes forward and 5 minutes backward in time, similar to what was done with the CML wet periods.

https://doi.org/10.5194/egusphere-2024-2625
Preprint. Discussion started: 18 September 2024

2.3 Disdrometer data and co-located CMLs

As reference data for the true precipitation type, we used disdrometer data from the Norwegian road authorities. They use two types of disdrometers, namely the OTT Parsivel and OTT Parsivel^2. The disdrometer data was downloaded from Frost (2024), a data hosting platform for meteorological observations run by the Norwegian Meteorological Institute. This dataset also contains precipitation type observations from sensors other than disdrometers, such as the Vaisala PWD12/31 and DRD11A. To ensure a more controlled comparison between sensors, we removed data from non-disdrometer sensors, using a registry provided by the road authorities. The disdrometers are placed at least 4 meters above the road at automated meteorological stations located along the roads in Norway and provide an estimate of the precipitation type every 10 minutes. The disdrometer precipitation is classified as light rain, rain, snow, and hail. No precipitation or dry weather is denoted *dry* in the following. We simplified this classification by merging the classes light rain and rain since they should appear similar in the CML and radar. Further, as there were few hail events in the dataset (less than 0.01%), we set time steps where the disdrometer recorded hail to dry. Thus from the simplifications the disdrometer only records 3 classes: dry, rain and snow. Pairs of CMLs and disdrometers within 8 km of each other were identified using methods from poligrain (2024) and CMLs longer than 8 km were removed. This resulted in 550 CMLs and 113 co-located disdrometers for December 2021 and 435 CMLs and 74 co-located disdrometers for June 2020. We refer to these as the winter and summer datasets respectively. The CMLs used in the study had lengths ranging from 0.4 to 8 km and operated at frequencies between 10 to 40 GHz, with the majority (90 percent) operating above 18 GHz.

2.3.1 Temperature, humidity and dew point temperature

Temperature and humidity data was downloaded from THREDDS (2024). The data is a downscaled version of ERA5 data on a 1 km grid with a temporal resolution of 1 hour (MET, 2024; Lussana et al., 2021, 2019). For each CML, we extracted the temperature and humidity at the midpoint of the CML. To account for air humidity we calculated the dew point temperature using the approximated relation with air temperature provided by Lawrence (2005), given as

$$T_d = T_a - ((100 - RH)/5), \tag{1}$$

where T_d is the dew point temperature, T_a is the air temperature and RH is the relative humidity.

2.4 Classification of rain and snow using the radar-temperature (RT) and CML-radar (CR) methods

The first method "radar-temperature" (RT), uses surface temperature and weather radar to determine precipitation occurrence and precipitation type. As recommended by Harder and Pomeroy (2014), humidity is accounted for by using the dew point temperature. The RT method then works by classifying radar precipitation above a dew point temperature threshold as rain and below the threshold as snow. In line with Marks et al. (2013) the dew point temperature threshold is set to 0 °C. Combining humidity-corrected temperature models with weather radar is a common method and is often used as a reference method (Casellas et al., 2021; Saltikoff et al., 2015; Gjertsen and Ødegaard, 2005). The second method, "CML-radar" (CR), uses the CML wet periods as an indicator for whether it is raining or not. Since the CML is not noticeably attenuated by dry snow we

https://doi.org/10.5194/egusphere-2024-2625
Preprint. Discussion started: 18 September 2024

Table 1. Radar and CML conditions and the CR method predictions

	Radar rain	**Radar dry**
CML rain	Rain	Rain
CML dry	Snow	Dry

can set radar precipitation that is not accompanied by CML precipitation as snow. The CR method predictions is summarized in Table 1.

2.5 Performance metrics

We use the Matthews correlation coefficient (MCC) to quantify the performance of the classification methods. The MCC is a statistical measure that provides a balanced evaluation metric, yielding 1 for a perfect estimate, 0 if the estimate are no better than random guesses, and -1 for complete disagreement between estimate and observation (Chicco and Jurman, 2020). In this study, we evaluated 3 classes, dry, rain and snow, making this a multiclass problem. For evaluating the classification of rainfall alone (MCC_rain), we considered two classes, rain or no rain. Thus for MCC_rain, dry and snow are in the same category. Likewise for snow (MCC_snow), dry and rain are in the same category. For the combined classes (MCC_all) we compute the multiclass MCC for all three categories, dry, rain and snow. The MCC_all, MCC_rain and MCC_snow were computed using *scikit-learn* (Pedregosa et al., 2011) which in the multiclass case implements MCC based on Gorodkin (2004).

2.6 Practical application investigating road friction

As a practical application, we studied how road friction, as measured at a meteorological station operated by the Norwegian road authorities, was related to the predictions from CR and RT methods. The meteorological station is located at Hålogalandsbrua bridge close to Narvik and the CML is located within 5 km distance to the meteorological station. We studied 11 days of data where the meteorological station recorded a broad range of weather events. The data from the road authorities included road condition as measured by a Vaisala remote surface state sensor DSC211, precipitation type as measured by a OTT Parsivel^2, the road temperature as measured by a Vaisala remote road surface temperature sensor DST111 and road friction as measured by a Vaisala remote surface state sensor DSC211. Road friction is rated from 0 to 1, typically at 0.82 for dry roads, 0.7 for wet roads, and between 0.4 to 0.6 for snowy or icy roads. No pre-processing of these data was performed.

3 Results

3.1 Overview of the data as a function of dew point temperature

Our dataset consists of CML-disdrometer pairs from the summer dataset and the winter dataset. Every minute each pair provides several different observations such as disdrometer observed precipitation type, dew point temperature and CML signal loss. In Fig. 1 we have plotted histograms of the number of minutes (first row), the observed disdrometer precipitation type (second row)

https://doi.org/10.5194/egusphere-2024-2625
Preprint. Discussion started: 18 September 2024

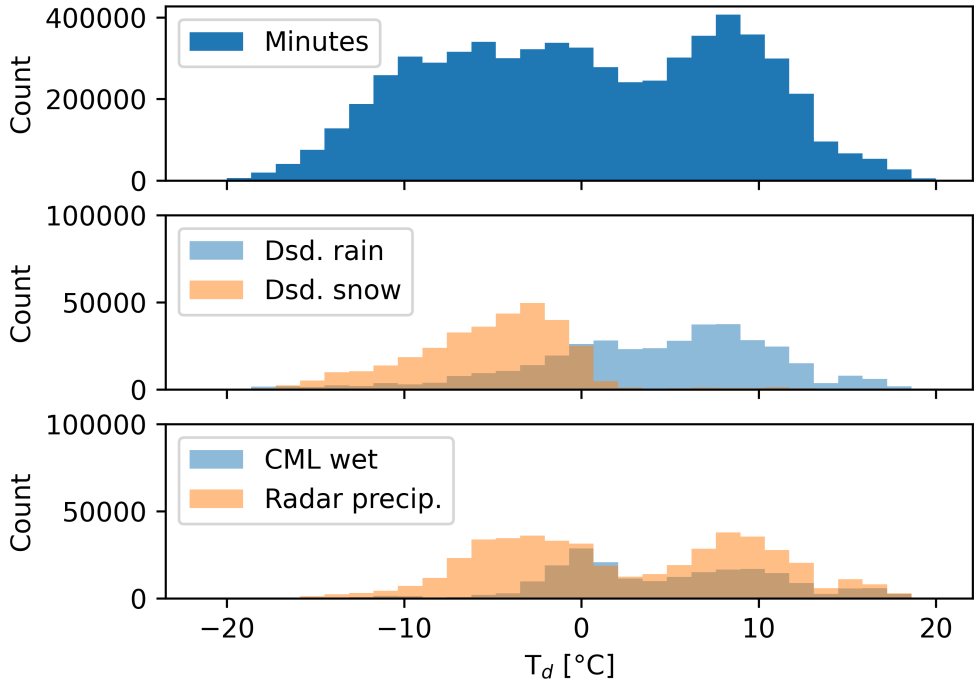

Figure 1. Frequency (counts of minutes) as a function of dew point temperature (T_d) for number of recordings (first row), disdrometer recorded rain and snow (second row) and CML recorded rain and radar recorded precipitation (third row).

and CML and radar precipitation (third row) for dew point temperature intervals of 1 degree between -20 and 20 degrees. From the disdrometer observations we can observe that all of our data is between -20 and 20 degrees with most of the observations concentrated between -10 and 10 degrees. The disdrometers record snow mainly below zero degrees with some recorded snow events slightly above zero degrees. For disdrometer rainfall, most rainfall is above zero degrees, but there is also a substantial amount of rainfall recorded below. The CML also detects wet precipitation below zero degrees, but not as frequently as the disdrometers. The weather radar detects more wet minutes around 10 degrees compared to the CML but it records fewer snowy minutes around -10 degrees compared to the disdrometer. We can also observe that the weather radar detects fewer events below -10 degrees as compared to the disdrometer.

3.2 The performance of the CR method vs. the RT method

The performance of the RT and CR method is visualized in scatter density plots using monthly time series for each CML-disdrometer pairs (Fig. 2). We can observe that for MCC_snow both methods perform quite similarly, while for MCC_rain CR seems to perform on average better than RT. For the combined classification the MCC_all is similar for both high RT and high CR scores, while for lower RT scores CR performs better. Looking at the mean dew point temperature we can observe that for

https://doi.org/10.5194/egusphere-2024-2625
Preprint. Discussion started: 18 September 2024

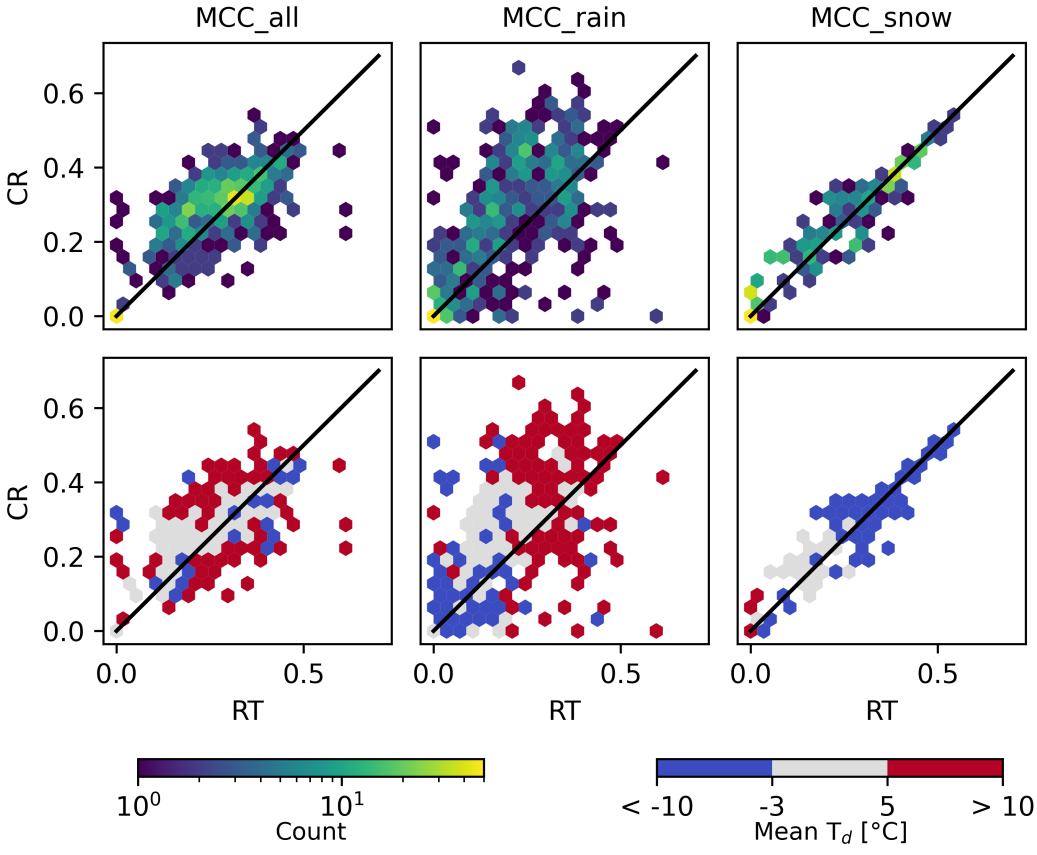

Figure 2. First row: Scatter density plots comparing the MCC_all, MCC_rain and MCC_snow of the CML based classification method CR and the reference method RT using the disdrometers as reference. The MCCs are computed for each CML-disdrometer pairs using 1 month of data. Second row: Same scatter density plots, but the cells show the mean dew point temperature (T_d) of each cell.

MCC_all and MCC_rain there is a gray cluster above the black line, indicating that the CR method in general improves the estimates for CMLs with a monthly mean temperature around zero degrees. Moreover, rainfall classification has a poorer score at lower average temperatures and snow classification has a poorer score at higher temperatures.

The MCC for all classes (MCC_all), for the rainfall class only (MCC_rain) and for the snow class only (MCC_snow) is plotted as a function of dew point temperature between -10 and 10 degrees (Fig. 3). We can observe that for the multiclass MCC_all both the CR and RT methods perform similar for low dew point temperature and high dew point temperature, while the CR method is superior in the dew point temperature range -1 to 7 degrees.

https://doi.org/10.5194/egusphere-2024-2625
Preprint. Discussion started: 18 September 2024

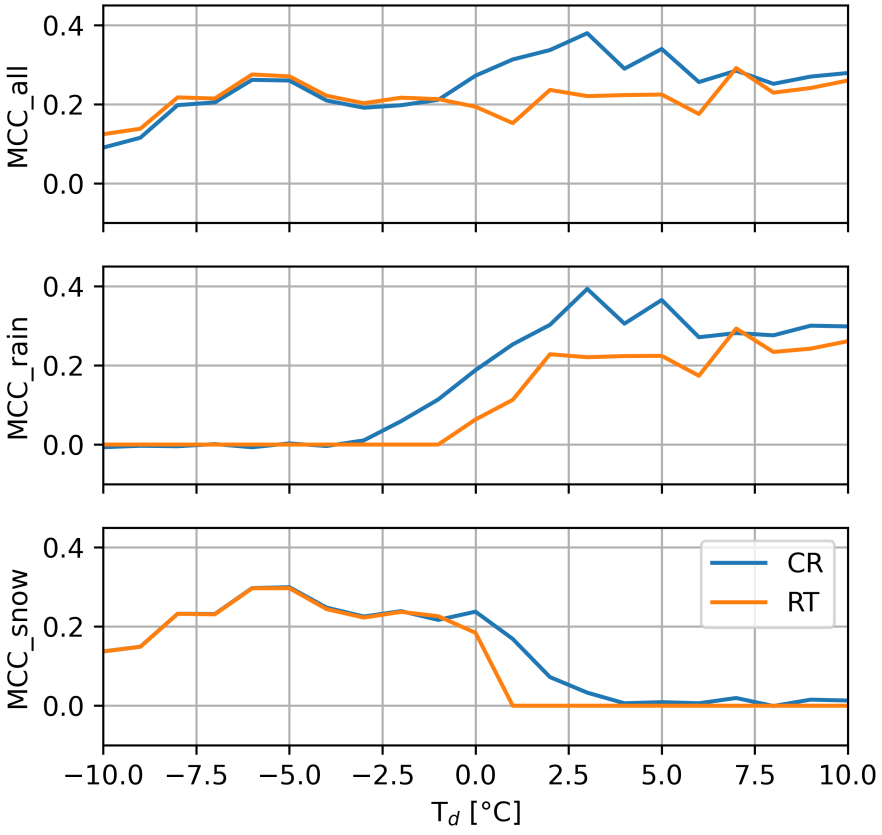

Figure 3. Matthews correlation coefficient for snow and rain (MCC_all), for rain (MCC_rain) and snow (MCC_snow) as a function of dew point temperature (T_d).

3.3 Precipitation bias as a function of temperature

The difference between the estimated CML rainfall amounts and the ground truth radar rainfall amounts is plotted as a function of dew point temperature (Fig. 4). The CML rainfall amounts were computed by using the weather radar wet period (left column) and by using the CML wet period (right column). For dew point temperature below -2 degrees, we observe that there is a positive bias where the radar in general overestimates the precipitation amounts compared to the CML. For dew point temperature around zero degrees, there seem to be many more events where there is a negative bias, meaning that the CML overestimates the rainfall amounts compared to the radar. For dew point temperature above 4 degrees, the CML and radar estimate has a similar spread. When using the CML to identify wet and dry periods, we more often observe a large negative bias compared to when the radar is used to identify wet and dry periods. In the second, third and fourth row, we have plotted

https://doi.org/10.5194/egusphere-2024-2625
Preprint. Discussion started: 18 September 2024

the fraction of hours within the bins where the disdrometer recorded at least 10 minutes of rain, snow and both snow and rain (mix) respectively. We observe that there is a lot of rain in observations above zero degrees, while there is a lot of snow in observations below zero degrees. Around zero degrees, we have observations of both rain and snow, and some hours where both rain and snow have been observed. We can also observe that for rainfall there is a larger proportion of the cells that experience more than 10 minutes of rainfall for negatively biased events, where the CML estimates more rainfall compared to the radar.

3.4 Map of CR and RT precipitation estimates

Fig. 5 displays a map showing the precipitation type estimated at the CML locations using the RT method (left column), the CR method (middle column) and the disdrometer observations (right column) for 1 hour accumulation periods. The RT method estimates rain (CML rain) if the weather radar observed rainfall for more than 5 minutes while the dew point temperature was positive, snow if the weather radar observes precipitation for more than 5 minutes while the dew point temperature was negative (CML snow), mix if both rain and snow was recorded for more than 5 minutes (CML mix) and no precipitation otherwise (CML dry). The CR method estimates rain when the CML recorded more than 5 minutes of rainfall (CML wet), snow when the radar recorded rainfall while the CML did not for more than 5 minutes (CML snow), mix if both rain and snow was recorded for more than 5 minutes (CML mix) and dry otherwise (CML dry). The disdrometers estimate rain when more than 10 minutes of rain is recorded (Dsd. rain), snow when more than 10 minutes of snow is recorded (Dsd. snow), mix when both rain and snow are recorded (Dsd. mix), and dry conditions otherwise (Dsd. dry).

Overall we can observe that in the south part of the map both the CR and RT method gives similar estimates, while in the middle and north the CR and RT method estimate a mixture of rain and snow. Looking at the CMLs located around point A (black cross) we can observe that in the first three time steps the RT method estimates more rainfall while the CR method estimates more mixed precipitation and the disdrometers observe mixed precipitation. In the forth time step both RT and CR estimates rain, snow and mix, while the disdrometers observe snow and mix. In the last time step the RT method estimates rainfall, the CR method estimates more snow and the disdrometers observes mostly snow.

3.5 Precipitation type and road friction

In a practical application of our study, we analyzed CML data and weather radar data at the CML location. This data was then compared with observations from a meteorological station in Narvik (Fig. 6). Looking at the CML time series (TL), we observe that around the 12th, the CML does not indicate any rainfall, while the radar observes precipitation and the disdrometer observes snow. Simultaneously, the road condition indicates snow and road friction drops rapidly. This suggests that the observed precipitation consists of dry snow, which is likely responsible for the reduction in road friction. Moving to the next event, we can observe that the road friction drops again between the 13th and 14th, but there is no recorded precipitation from either the radar or the disdrometers. From the road condition, we can observe that the road has transitioned from damp to ice, indicating that the road friction is low due to water that has frozen. Next, between the 15th and 16th, there is a drop in the road friction where the disdrometers and road condition indicate snow. However, the CML indicates a wet period. Comparing the difference between the CML and weather radar we see that the CML overestimates rainfall by more than 5 mm for those hours. Looking

https://doi.org/10.5194/egusphere-2024-2625
Preprint. Discussion started: 18 September 2024

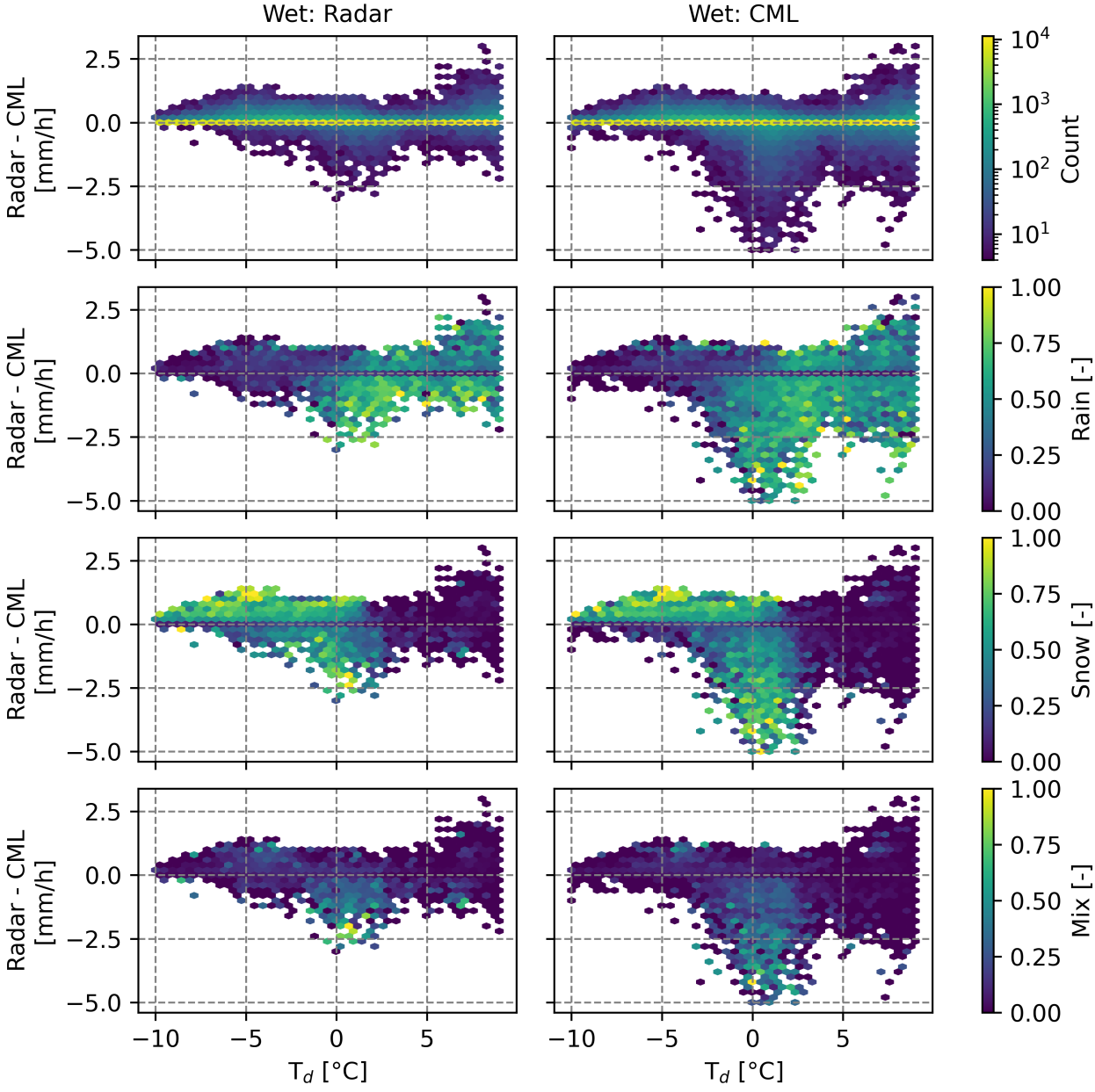

Figure 4. First row: Difference between hourly precipitation amounts as measured by radar and CML as a function of dew point temperature (T_d). CML rain amounts were estimated using wet periods identified by the weather radar (left column) and the CML (right column). Second, third, and fourth row: The fraction of the hours within the bins where the disdrometer recorded at least 10 minutes of rainfall, snow, and both snow and rain (mixed precipitation), respectively. Cells with less than 4 events are not shown.

https://doi.org/10.5194/egusphere-2024-2625
Preprint. Discussion started: 18 September 2024

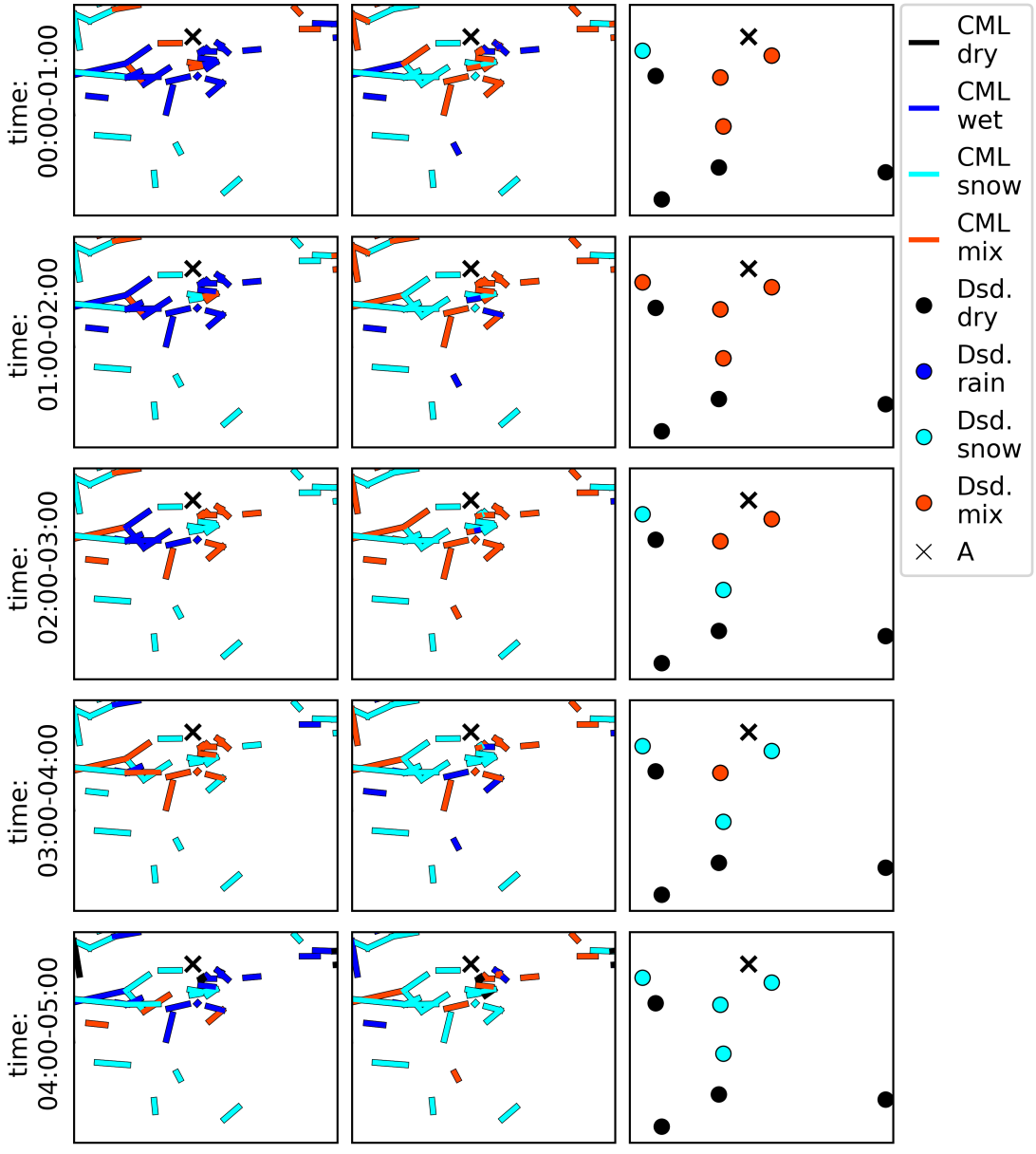

Figure 5. A 50 x 100km area in Norway observed in 1-hour intervals from 00:00 to 04:00 on 19th December 2021. The left column show the CML condition using the RT method, the middle column show the CML condition using the CR method and the right column show the disdrometer observations. The colors reflect the estimated weather conditions dry (black), rainy (blue), snowy (cyan) and dry (red). The black x indicates point A for orientation. Coordinates are not shown due to data security reasons.

https://doi.org/10.5194/egusphere-2024-2625
Preprint. Discussion started: 18 September 2024

at the TL of the CML we observe that the TL has a more gradual increase, not like the more variable pattern seen at the next time steps where the disdrometer and road condition indicate that it is raining. Given that the disdrometers indicate snow and the CML indicates a wet period, this could suggest that the decreased road friction is caused by wet snow. Interestingly, this event caused a larger drop in road friction than the two previous events on the 12th and 14th. After this event, the disdrometer and road condition indicate a long rainy period between the 16th and 19th. This is supported by the CML and radar estimating approximately the same amounts of rainfall. Just before the 19th, there is a short period where the CML overestimates rainfall amounts and the disdrometer records snow. However, the period is so short that the road friction is not dropping. Finally, between the 19th and 20th, there is a large drop in road friction where the CML also overestimates rainfall amounts compared to the radar, and the disdrometer records snow. This could again indicate that the decreased road friction is caused by wet snow.

Fig. 6 also shows that during the rainy period between the 16th and 19th, the CR method estimates switches more between rain and snow compared to the RT method. This could be due to that there is a mixture of snow and rain at temperatures close to zero degrees. It could also be that the CML and weather radar are not perfectly synchronized, causing the CR method to predict snow for instance when the weather radar detects rainfall shortly before the CML.

4 Discussion

4.1 The distribution of rain and snow around zero degrees

The disdrometer data suggest that there is more frequent rainfall below zero degrees than there is snow above zero degrees (Fig. 1). Although there is no reason to expect that the distribution of rain and snow around zero degrees should be symmetric, observing significant rainfall amounts far below zero degrees is not expected. Comparing the CML wet distribution with the disdrometer rain distribution, we can see that the CML observes fewer wet events below zero degrees. We have also observed that snow events around zero degrees can show up as wet in the CML (Fig. 4). Thus, contrary to what we observe, below zero degrees we should expect that the CML estimates more wet events than the disdrometer observes rainfall. This could indicate that the disdrometers overestimate the number of rainy events below zero degrees. One reason for this overestimation could be due to the spatial distance between the disdrometer and the CML midpoint where the temperature is recorded. Since the temperature can be different at those locations due to for instance differences in elevation, we should expect that some rain events are assigned to colder temperatures while others are assigned to warmer temperatures. On the other hand, if this effect played a large role we should also see the same effect for snow, with more snow being recorded up to 10 ∘C. Another explanation could be that wet snow makes the disdrometer alternate between snow and rain, with a stronger emphasis in rain, creating the impression that there is more rain below zero degrees. Other explanations could be errors in the disdrometer classification algorithm or it could come from cars spraying water droplets from salted roads. Consequently, while the disdrometer provides valuable estimates, it may not perfectly represent the ground truth.

https://doi.org/10.5194/egusphere-2024-2625
Preprint. Discussion started: 18 September 2024

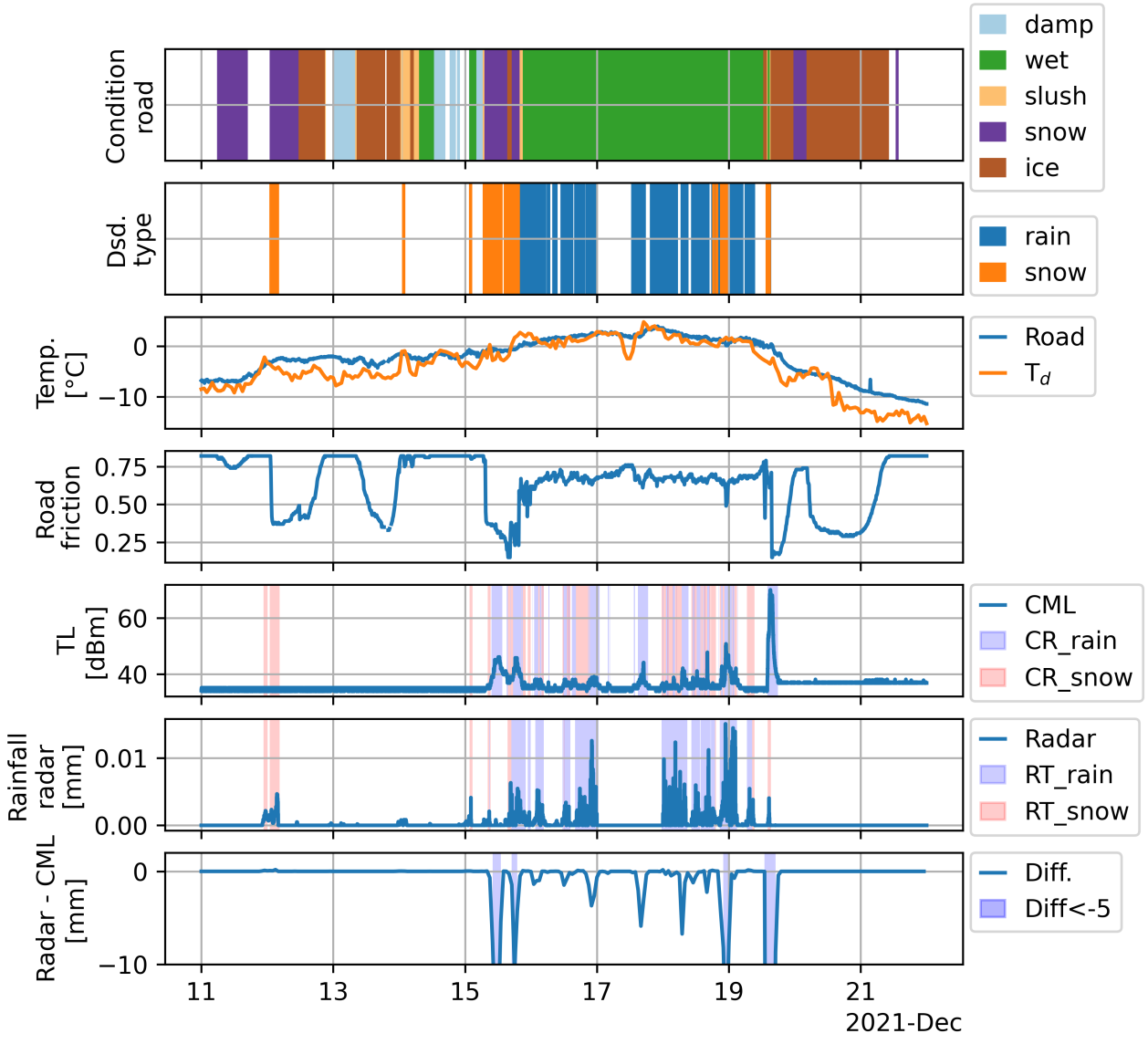

Figure 6. Time series for the meteorological station in Narvik operated by the Norwegian road authorities. The first row shows the road condition dry (white), damp (light blue), wet (green), slush (orange), snow (purple) and ice (brown). The next row shows whether the disdrometer records no (white), liquid (blue) or solid (orange) precipitation. The third row shows the dew point temperature (orange) and the temperature measured by a sensor mounted next to the road (blue). The fourth row shows the road friction as measured by a sensor in the road. The fifth row shows the total loss of a nearby CML (TL) as well as the estimated wet (blue) and snowy (red) periods using the CR method. The sixth row shows the radar precipitation amounts (blue line) measured as a weighted sum along the CML as well as snowy (red shade) and rainy (blue shade) periods as estimated by the RT method. The seventh row shows the difference between the radar and CML rainfall amounts (blue line) as well as the time steps where the difference is less than -5 (blue shade).

https://doi.org/10.5194/egusphere-2024-2625
Preprint. Discussion started: 18 September 2024

4.2 CML dry periods can be used in combination with weather radar to classify dry snow

Below -1 degrees the CR method is able to classify snow with a similar accuracy as the RT method. For temperatures above -1 degrees both the CR and RT method performance decreases, but the CR performance decreases slower than the RT method, indicating an advantage of using the CR method for classifying snow (Fig. 3). Part of the performance decrease of the CR method could be due to that at higher temperatures the spatial differences between the CML and disdrometer plays a larger role. For instance, the chance for rain at the disdrometer is (naturally) higher for higher temperatures (ca.5°C) than for lower temperatures (-10°C), even if it may be snowing at the CML location in both cases. Other explanations for the CR method performance decrease could be that the disdrometers classify wet snow as snow, while the CMLs classify wet snow as rainfall, leading to a misclassification by the CMLs. This phenomenon is clearly observable in Fig. 6 where all events featuring CML overestimation of rainfall amounts coincide with the disdrometer recording snow. A similar pattern is evident in Figure 4, where instances of large CML bias around zero degrees often correspond with the disdrometer measuring snow or a combination of rain and snow. This suggests that events characterized by wet snow are likely to be classified as wet by the CML wet classification method. We also experimented with other CML wet classification methods and found the same results. This indicates that even if we are able to classify dry snow better using the CMLs and weather radar, we might fail at classifying wet snow. Future work could investigate methods for wet snow detection, for instance, by looking at the difference between the radar estimate and the CML estimate or by refining and testing the method proposed by Cherkassky et al. (2014) on a larger dataset.

4.3 CMLs improve rainfall detection

In terms of rainfall classification, the CR method performs just as well or outperforms the RT method for all temperature ranges (Fig. 2 and Fig. 3). This could be due to the fact that the CMLs are located on the ground, which situates them closer to the disdrometers compared to the radar beam. Alternatively, the improved accuracy could be due to radar beam blockage by mountains causing insufficient coverage at some locations. We note that the RT method uses the CML geometry to estimate the radar rainfall and that it could be improved by using the pixel value at the position of the disdrometer. This was done to make the CR and RT methods have the same spatial differences as the disdrometer, making them more comparable. Finally, we can also observe that the performance of the CR method is lower at -1 degrees than at 3 degrees (Fig. 3). This could be due to the fact that at temperatures below -1 degrees, there are more mixed events where the disdrometer records snow and the CML estimates rainfall.

4.4 Wet snow causes significant discrepancies between CML and radar estimates around zero degrees

Around zero degrees the CML estimates larger rainfall amounts compared to the radar (Fig. 4). This effect has been observed before in previous studies, for instance in Graf et al. (2020), where the authors noted a marked discrepancy between CML and radar readings during the winter months, potentially induced by wet snow. Many of the significant discrepancies between the radar and CML estimate coincide with hours during which a mix of rain and snow events were recorded (Fig. 4). This suggests

https://doi.org/10.5194/egusphere-2024-2625
Preprint. Discussion started: 18 September 2024

that significant discrepancies between the CML and radar estimates around zero degrees may be attributed to wet snow. From 4°C upwards, both the radar and CMLs provide similar spread in rainfall amount estimates, indicating a balanced comparison at these temperatures. This suggests that there is less discrepancy or bias between CML and radar rainfall rate measurements when the dew point temperature is above 4°C.

4.5 Nearby CMLs can be used to interpret road friction

In Fig. 6 we can observe that strong snow events causes the road friction to drop. This occurs, for instance, around the 12th, when the disdrometer observes snow. The strongest drop in road friction appears to coincide with instances where both the CML indicates rainfall and the disdrometer registers snow. During these events there is also a significant discrepancy between the weather radar and the CML estimates. This discrepancy can, as previously discussed, be caused by wet snow, suggesting that the pronounced decrease in road friction might be attributed to conditions of wet snow. However, for practical applications, it must be noted that road friction can also drop due to other factors, such as icy roads. Moreover, we can also observe that not all wet snow periods cause the road friction to drop. Reasons for this could be, for instance, that water on the road is causing wet snow to melt, a too short duration of the snow event, or that the snow was removed by the road authorities.

5 Conclusions

In this work, we have compared two methods for classifying rain and snow, one established reference method where we combine surface dew point temperature and weather radar (RT) and one novel method where we combine CMLs and weather radar (CR). The CR method exploits the fact that dry snow causes low signal attenuation of the CML signal level, making dry snow events appear similar to dry events in the CML time series. It works by classifying time steps where the weather radar detects precipitation and the CMLs do not detect precipitation. Time steps where the CML detects rainfall are set to wet. The RT method classifies weather radar precipitation below zero degrees as snow and above as rain. Our results show that the CR method outperforms the RT method for dry snow detection above zero degrees and, in general, for rainfall detection, suggesting that CMLs can be used to better classify rain and snow. Further, our results indicate that wet snow is classified as rainfall by the CML and that during these events the disdrometer tends to estimate a mix of rainfall and snow. These events are also characterized by large CML overestimations compared to radar, which could be attributed to the larger signal attenuation caused by wet snow. Overall, our findings suggest a new application for using CMLs to identify dry snow and contribute to better understanding on how CMLs behave during events of mixed precipitation.

Code and data availability. The software used for CML processing software is available under https://github.com/pycomlink/pycomlink/tree/master. Disdrometer data is available from (Frost, 2024). Radar data is available from (THREDDS, 2024). CML data is not available.

https://doi.org/10.5194/egusphere-2024-2625
Preprint. Discussion started: 18 September 2024

Author contributions. Conceptualization: EØ, JA, RB. Data curation: EØ. Methodology: EØ, JA, RG, RB, MW, NOK, CC, VN. Software: EØ, CC. Supervision: VN, MW, NOK, RB. Writing – original draft preparation: EØ. Writing – review and editing: EØ, RG, JA, RB, MW, NOK, CC, VN.

Competing interests. The contact author has declared that neither of the authors has any competing interests.

Acknowledgements. The authors thank co-supervisor Etienne Leblois for nice discussions. We would also like to thank Ericsson for providing CML data. This work is funded by the Norwegian University of Life Sciences and the German Research Foundation via the SpraiLINK project (Grant CH-1785/2-1).

https://doi.org/10.5194/egusphere-2024-2625
Preprint. Discussion started: 18 September 2024

References

Blettner, N., Fencl, M., Bareš, V., Kunstmann, H., and Chwala, C.: Transboundary Rainfall Estimation Using Commercial Microwave Links, Earth and Space Science, 10, https://doi.org/10.1029/2023EA002869, 2023.

Casellas, E., Bech, J., Veciana, R., Pineda, N., Miró, J. R., Moré, J., Rigo, T., and Sairouni, A.: Nowcasting the precipitation phase combining weather radar data, surface observations, and NWP model forecasts, Quarterly Journal of the Royal Meteorological Society, 147, 3135–3153, https://doi.org/10.1002/qj.4121, 2021.

Chandrasekar, V., Keränen, R., Lim, S., and Moisseev, D.: Recent advances in classification of observations from dual polarization weather radars, Atmospheric Research, 119, 97–111, https://doi.org/10.1016/j.atmosres.2011.08.014, 2013.

Cherkassky, D., Ostrometzky, J., and Messer, H.: Precipitation Classification Using Measurements From Commercial Microwave Links, IEEE Transactions on Geoscience and Remote Sensing, 52, 2350–2356, https://doi.org/10.1109/TGRS.2013.2259832, 2014.

Chicco, D. and Jurman, G.: The advantages of the Matthews correlation coefficient (MCC) over F1 score and accuracy in binary classification evaluation, BMC Genomics, 21, 6, https://doi.org/10.1186/s12864-019-6413-7, 2020.

Chwala, C., Polz, J., Graf, M., Sereb, D., Blettner, N., Keis, F., and Boose, Y.: pycomlink/pycomlink: v0.3.2, https://doi.org/https://doi.org/10.5281/ zenodo.4810169, 2023.

Elmore, K. L.: The NSSL Hydrometeor Classification Algorithm in Winter Surface Precipitation: Evaluation and Future Development, Weather and Forecasting, 26, 756–765, https://doi.org/10.1175/WAF-D-10-05011.1, 2011.

Feiccabrino, J. M.: Precipitation phase uncertainty in cold region conceptual models resulting from meteorological forcing time-step intervals, Hydrology Research, 51, 180–187, https://doi.org/10.2166/nh.2020.080, 2020.

Friedrich, K., Kalina, E. A., Masters, F. J., and Lopez, C. R.: Drop-Size Distributions in Thunderstorms Measured by Optical Disdrometers during VORTEX2, Monthly Weather Review, 141, 1182–1203, https://doi.org/10.1175/MWR-D-12-00116.1, 2013.

Frost: https://frost.met.no/index.html, 2024.

Førland, E., Allerup, P., Dahlström, B., Elomaa, E., Jónsson, T., Madsen, H., Perälä, J., Rissanen, P., Vedin, H., and Vejen, F.: Manual for Operational Correction of Nordic Precipitation Data, DNMI-report, Norske meteorologiske institutt, https://books.google.no/books?id=HLIKcgAACAAJ, 1996.

Gjertsen, U. and Ødegaard, V.: The water phase of precipitation—a comparison between observed, estimated and predicted values, Atmospheric Research, 77, 218–231, https://doi.org/10.1016/j.atmosres.2004.10.030, 2005.

Gorodkin, J.: Comparing two K-category assignments by a K-category correlation coefficient, Computational Biology and Chemistry, 28, 367–374, https://doi.org/10.1016/j.compbiolchem.2004.09.006, 2004.

Graf, M., Chwala, C., Polz, J., and Kunstmann, H.: Rainfall estimation from a German-wide commercial microwave link network: optimized processing and validation for 1 year of data, Hydrology and Earth System Sciences, 24, 2931–2950, https://doi.org/10.5194/hess-24-2931-2020, 2020.

Grazioli, J., Tuia, D., and Berne, A.: Hydrometeor classification from polarimetric radar measurements: a clustering approach, Atmospheric Measurement Techniques, 8, 149–170, https://doi.org/10.5194/amt-8-149-2015, 2015.

Harder, P. and Pomeroy, J.: Estimating precipitation phase using a psychrometric energy balance method, Hydrological Processes, 27, 1901–1914, https://doi.org/10.1002/hyp.9799, 2013.

Harder, P. and Pomeroy, J. W.: Hydrological model uncertainty due to precipitation-phase partitioning methods, Hydrological Processes, 28, 4311–4327, https://doi.org/10.1002/hyp.10214, 2014.

https://doi.org/10.5194/egusphere-2024-2625
Preprint. Discussion started: 18 September 2024

Harpold, A. A., Kaplan, M. L., Klos, P. Z., Link, T., McNamara, J. P., Rajagopal, S., Schumer, R., and Steele, C. M.: Rain or snow: hydrologic processes, observations, prediction, and research needs, Hydrology and Earth System Sciences, 21, 1–22, https://doi.org/10.5194/hess-21-1-2017, 2017.

ITU, R.: RECOMMENDATION ITU-R P.838-3 Specific attenuation model for rain for use in prediction methods, pp. 1–8, 2005.

Jennings, K. S., Winchell, T. S., Livneh, B., and Molotch, N. P.: Spatial variation of the rain–snow temperature threshold across the Northern Hemisphere, Nature Communications, 9, 1148, https://doi.org/10.1038/s41467-018-03629-7, 2018.

Kienzle, S. W.: A new temperature based method to separate rain and snow, Hydrological Processes, 22, 5067–5085, https://doi.org/10.1002/hyp.7131, 2008.

Kochendorfer, J., Earle, M., Rasmussen, R., Smith, C., Yang, D., Morin, S., Mekis, E., Buisan, S., Roulet, Y.-A., Landolt, S., Wolff, M., Hoover, J., Thériault, J. M., Lee, G., Baker, B., Nitu, R., Lanza, L., Colli, M., and Meyers, T.: How Well Are We Measuring Snow Post-SPICE?, Bulletin of the American Meteorological Society, 103, E370–E388, https://doi.org/10.1175/BAMS-D-20-0228.1, 2022.

Lamb, D. and Verlinde, J.: Physics and Chemistry of Clouds, Cambridge University Press, ISBN 9780521899109, https://doi.org/10.1017/CBO9780511976377, 2011.

Lawrence, M. G.: The Relationship between Relative Humidity and the Dewpoint Temperature in Moist Air: A Simple Conversion and Applications, Bulletin of the American Meteorological Society, 86, 225–234, https://doi.org/10.1175/BAMS-86-2-225, 2005.

Leijnse, H., Uijlenhoet, R., and Stricker, J. N. M.: Rainfall measurement using radio links from cellular communication networks, Water Resources Research, 43, 1–6, https://doi.org/10.1029/2006WR005631, 2007.

Leijnse, H., Uijlenhoet, R., and Stricker, J.: Microwave link rainfall estimation: Effects of link length and frequency, temporal sampling, power resolution, and wet antenna attenuation, Advances in Water Resources, 31, 1481–1493, https://doi.org/10.1016/j.advwatres.2008.03.004, 2008.

Leroux, N. R., Vionnet, V., and Thériault, J. M.: Performance of precipitation phase partitioning methods and their impact on snowpack evolution in a humid continental climate, Hydrological Processes, 37, https://doi.org/10.1002/hyp.15028, 2023.

Loth, B., Graf, H., and Oberhuber, J. M.: Snow cover model for global climate simulations, Journal of Geophysical Research: Atmospheres, 98, 10 451–10 464, https://doi.org/10.1029/93JD00324, 1993.

Lussana, C., Seierstad, I. A., Nipen, T. N., and Cantarello, L.: Spatial interpolation of two-metre temperature over Norway based on the combination of numerical weather prediction ensembles and in situ observations, Quarterly Journal of the Royal Meteorological Society, 145, 3626–3643, https://doi.org/10.1002/qj.3646, 2019.

Lussana, C., Nipen, T. N., Seierstad, I. A., and Elo, C. A.: Ensemble-based statistical interpolation with Gaussian anamorphosis for the spatial analysis of precipitation, Nonlinear Processes in Geophysics, 28, 61–91, https://doi.org/10.5194/npg-28-61-2021, 2021.

Löffler-Mang, M. and Joss, J.: An Optical Disdrometer for Measuring Size and Velocity of Hydrometeors, Journal of Atmospheric and Oceanic Technology, 17, 130–139, https://doi.org/10.1175/1520-0426(2000)017<0130:AODFMS>2.0.CO;2, 2000.

Marks, D., Winstral, A., Reba, M., Pomeroy, J., and Kumar, M.: An evaluation of methods for determining during-storm precipitation phase and the rain/snow transition elevation at the surface in a mountain basin, Advances in Water Resources, 55, 98–110, https://doi.org/10.1016/j.advwatres.2012.11.012, 2013.

Marshall, J. S. and Palmer, W. M. K.: The distribution of raindrops with size, Journal of Meteorology, 5, 165–166, https://doi.org/10.1175/1520-0469(1948)005<0165:TDORWS>2.0.CO;2, 1948.

Matsuo, T., Sasyo, Y., and Sato, Y.: Relationship between Types of Precipitation on the Ground and Surface Meteorological Elements, Journal of the Meteorological Society of Japan. Ser. II, 59, 462–476, https://doi.org/10.2151/jmsj1965.59.4_462, 1981.

https://doi.org/10.5194/egusphere-2024-2625
Preprint. Discussion started: 18 September 2024

McCabe, G. J., Clark, M. P., and Hay, L. E.: Rain-on-Snow Events in the Western United States, Bulletin of the American Meteorological Society, 88, 319–328, https://doi.org/10.1175/BAMS-88-3-319, 2007.

Messer, H., Zinevich, A., and Pinhas, A.: Environmental Monitoring by Wireless Communication Networks, Science, 312, 17–18, https://www.jstor.org/stable/3846088, 2006.

MET: MET Nordic dataset, https://github.com/metno/NWPdocs/wiki/MET-Nordic-dataset, 2024.

Nešpor, V. and Sevruk, B.: Estimation of Wind-Induced Error of Rainfall Gauge Measurements Using a Numerical Simulation, Journal of Atmospheric and Oceanic Technology, 16, 450–464, https://doi.org/10.1175/1520-0426(1999)016<0450:EOWIEO>2.0.CO;2, 1999.

Ostrometzky, J., Cherkassky, D., and Messer, H.: Accumulated Mixed Precipitation Estimation Using Measurements from Multiple Microwave Links, Advances in Meteorology, 2015, 1–9, https://doi.org/10.1155/2015/707646, 2015.

Overeem, A., Leijnse, H., and Uijlenhoet, R.: Country-wide rainfall maps from cellular communication networks, Proceedings of the National Academy of Sciences, 110, 2741–2745, https://doi.org/10.1073/pnas.1217961110, 2013.

Overeem, A., Leijnse, H., and Uijlenhoet, R.: Two and a half years of country-wide rainfall maps using radio links from commercial cellular telecommunication networks, Water Resources Research, 52, 8039–8065, https://doi.org/10.1002/2016WR019412, 2016.

Pastorek, J., Fencl, M., and Bareš, V.: Uncertainties in discharge predictions based on microwave link rainfall estimates in a small urban catchment, Journal of Hydrology, 617, 129 051, https://doi.org/10.1016/j.jhydrol.2022.129051, 2023.

Paulson, K. and Al-Mreri, A.: A rain height model to predict fading due to wet snow on terrestrial links, Radio Science, 46, https://doi.org/10.1029/2010RS004555, 2011.

Pedregosa, F., Varoquaux, G., Gramfort, A., Michel, V., Thirion, B., Grisel, O., Blondel, M., Prettenhofer, P., Weiss, R., Dubourg, V., Vanderplas, J., Passos, A., Cournapeau, D., Brucher, M., Perrot, M., and Duchesnay, E.: Scikit-learn: Machine Learning in Python, Journal of Machine Learning Research, 12, 2825–2830, 2011.

poligrain: Poligrain, https://github.com/OpenSenseAction/poligrain, 2024.

Polz, J., Chwala, C., Graf, M., and Kunstmann, H.: Rain event detection in commercial microwave link attenuation data using convolutional neural networks, Atmospheric Measurement Techniques, 13, 3835–3853, https://doi.org/10.5194/amt-13-3835-2020, 2020.

Pu, K., Liu, X., Hu, S., and Gao, T.: Hydrometeor Identification Using Multiple-Frequency Microwave Links: A Numerical Simulation, Remote Sensing, 12, 2158, https://doi.org/10.3390/rs12132158, 2020.

Saltikoff, E., Lopez, P., Taskinen, A., and Pulkkinen, S.: Comparison of quantitative snowfall estimates from weather radar, rain gauges and a numerical weather prediction model, Boreal Environment Research, 20, 2015.

Schleiss, M., Rieckermann, J., and Berne, A.: Quantification and Modeling of Wet-Antenna Attenuation for Commercial Microwave Links, IEEE Geoscience and Remote Sensing Letters, 10, 1195–1199, https://doi.org/10.1109/LGRS.2012.2236074, 2013.

Stewart, R. E.: Precipitation Types in the Transition Region of Winter Storms, Bulletin of the American Meteorological Society, 73, 287–296, https://doi.org/10.1175/1520-0477(1992)073<0287:PTITTR>2.0.CO;2, 1992.

Stewart, R. E., Thériault, J. M., and Henson, W.: On the Characteristics of and Processes Producing Winter Precipitation Types near 0°C, Bulletin of the American Meteorological Society, 96, 623–639, https://doi.org/10.1175/BAMS-D-14-00032.1, 2015.

THREDDS: https://thredds.met.no/thredds/catalog.html, 2024.

Wolff, M. A., Isaksen, K., Petersen-Øverleir, A., Ødemark, K., Reitan, T., and Brækkan, R.: Derivation of a new continuous adjustment function for correcting wind-induced loss of solid precipitation: results of a Norwegian field study, Hydrology and Earth System Sciences, 19, 951–967, https://doi.org/10.5194/hess-19-951-2015, 2015.

https://doi.org/10.5194/egusphere-2024-2625
Preprint. Discussion started: 18 September 2024

Yuter, S. E., Kingsmill, D. E., Nance, L. B., and Löffler-Mang, M.: Observations of Precipitation Size and Fall Speed Characteristics within Coexisting Rain and Wet Snow, Journal of Applied Meteorology and Climatology, 45, 1450–1464, https://doi.org/10.1175/JAM2406.1, 2006.

Øydvin, E., Graf, M., Chwala, C., Wolff, M. A., Kitterød, N.-O., and Nilsen, V.: Technical Note: A simple feedforward artificial neural network for high temporal resolution classification of wet and dry periods using signal attenuation from commercial microwave links, EGUsphere [preprint], https://doi.org/https://doi.org/10.5194/egusphere-2024-647, 2024.